

## Electronic Supplementary Information

### Shape Selectivity Extending to Ordered Supermicroporous Aluminosilicates

Wen Hua Fu <sup>a</sup>, Xiao Min Liang <sup>a</sup>, Haidong Zhang <sup>b,\*</sup>, Yi Meng Wang <sup>a,\*</sup>, Ming Yuan He <sup>a</sup>

<sup>a</sup> *Shanghai Key Lab of Green Chemistry and Chemical Processes, Department of Chemistry, East China Normal University, Shanghai 200062, PR China; Tel: +86-21-62232251; fax: 0086-21-62232251; E-mail: [ymwang@chem.ecnu.edu.cn](mailto:ymwang@chem.ecnu.edu.cn)*

<sup>b</sup> *Engineering research centre of waste oil recovery technology and equipment of Chinese ministry of education, Chongqing Key laboratory of catalysis science and technology, Chongqing Technology and Business University, Chongqing 400067, PR China, Fax: +86-23-62768317, E-mail: [haidongzhang@ctbu.edu.cn](mailto:haidongzhang@ctbu.edu.cn)*

## Contents:

### Experimental

Synthesis of catalysts

Characterization and theoretical calculation models

Reaction tests

**Fig. S1** CH<sub>3</sub>O(CH<sub>2</sub>O)<sub>5</sub>CH<sub>3</sub> model optimized using Gaussian 09.

**Fig. S2** XRD patterns of the catalysts.

**Fig. S3** NH<sub>3</sub>-TPD profiles of aluminosilicate catalysts: (a) USY-1, (b) USY-3 (60), (c) C<sub>10</sub>-AS-50, and (d) C<sub>16</sub>-Al-SBA-1.

**Fig. S4** Typical transmission electron microscopy (TEM) images of C<sub>10</sub>-AS-50.

**Fig. S5** Product distribution versus the *n* value in PODE<sub>*n*</sub> by using different catalysts.

**Fig. S6** Recyclability studies of C<sub>10</sub>-AS-50 catalyst in the synthesis of PODE<sub>*n*</sub>

**Table S1** Physical properties of conventional diesel fuel (CDF), methylal and polyoxymethylene dimethyl ethers (PODE<sub>*n*</sub>).

**Table S2** PODE<sub>*n*</sub> product distribution by using different catalysts.

**Table S3** The optimized models of PODE<sub>3</sub>, PODE<sub>5</sub> and PODE<sub>8</sub> by Gaussian 09.

### References

## Experimental

### Synthesis of catalysts

The ordered supermicroporous aluminosilicate with *Pm3n* symmetry was prepared as described in our previous work.<sup>1</sup> In a typical synthesis, the surfactant decyltrimethylammonium bromide (C<sub>10</sub>TMAB) and aluminum sulfate (Al<sub>2</sub>(SO<sub>4</sub>)<sub>3</sub>·18H<sub>2</sub>O) were dissolved into water, followed by acidification of the solution with sulfuric acid. The solution was then precooled at 273 K for 30 min. Under stirring, tetraethyl orthosilicate (TEOS) was added and hydrolyzed for about 1 h to ensure the mixture turned into a transparent solution. A solution of ammonia (25 %) was then poured into the solution and precipitate began to emerge. After stirring at 273 K for another 24 h, the precipitate was filtered, washed with deionized water, dried at 373 K overnight and calcined at 823 K for 5 h to remove the template. The molar composition of the mixture was 0.50 C<sub>10</sub>TMAB : 1.0 TEOS : 0.11 H<sub>2</sub>SO<sub>4</sub> : 0.02 Al<sub>2</sub>(SO<sub>4</sub>)<sub>3</sub> : 4.5 NH<sub>3</sub> : 500 H<sub>2</sub>O. The catalyst was denoted as C<sub>10</sub>-AS-50, where AS was short for aluminosilicate and 50 was the molar ratio of SiO<sub>2</sub>/Al<sub>2</sub>O<sub>3</sub> in the initial synthesis gel.

For comparison, three other catalysts with different pore diameters were also used. Catalyst C<sub>16</sub>-Al-SBA-1 was prepared by grinding an as-prepared C<sub>16</sub>-SBA-1 silica/surfactant composite with aluminum nitride (Al(NO<sub>3</sub>)<sub>3</sub>·9H<sub>2</sub>O) for *ca.* 15 min, followed by the calcination at 823 K for 5 h. The C<sub>16</sub>-SBA-1 material was synthesized as reported in Kim's work.<sup>2</sup> In a typical synthesis of C<sub>16</sub>-SBA-1, 6.5 g cetyltriethylammonium bromide (C<sub>16</sub>TEAB) was dissolved into 143.5 g deionized water. 57.6 g concentrated hydrochloric acid (36.5 % HCl) was added and the solution was cooled in an alcohol bath at 273 K for 30 min. 16.6 g tetraethyl orthosilicate (TEOS) was added under stirring and the reaction was carried out at 273 K for another 24 h. After that, the precipitate was filtered, dried at ambient temperature and 373 K overnight, sequentially.

The USY-1, USY-3 zeolites used in this work were purchased from from Huahua Group Co., Ltd., Wenzhou, China. USY-3 (60) was obtained by dealumination of the parent USY-3 zeolite with 0.6 M HNO<sub>3</sub> at 353 K for *ca.* 30 min.

### Characterization and theoretical calculation models

Powder X-ray diffraction (XRD) patterns were recorded on a Rigaku-Ultima

diffractometer, with Cu K $\alpha$  radiation at 35 kV and 25 mA. Nitrogen sorption isotherms were measured on a BELSORP-max volumetric adsorption analyzer. The samples were outgassed at 573 K for 6 h before measurement. The Brunauer- Emmett-Teller (BET) specific surface area was calculated using adsorption data acquired at a relative pressure ( $p/p_0$ ) range of 0.01–0.1 and the total pore volume determined from the amount adsorbed at a relative pressure of about 0.99. The pore size diameters were calculated from the analysis of adsorption branch of the isotherm using the Barrett–Joyner–Halenda (BJH) algorithm and non-local density functional theory (NLDFT) algorithm. Inductively coupled plasma atomic emission spectrometry (ICP-AES) was recorded on a Thermo IRIS Intrepid II XSP atomic emission spectrometer after dissolving the samples in HF solution. Temperature-programmed desorption of NH<sub>3</sub> (NH<sub>3</sub>-TPD) testing was performed using a TP-5080 chemisorption instrument (Xianquan Co., Ltd, Tianjin, China) with a thermal conductivity detector (TCD). After pretreatment at 550 °C under flowing helium (25 mL/min) for 1 h, each sample (100 mg) was cooled to 100 °C, and then adsorbed to saturation by ammonia for 30 minutes. Ammonia physically adsorbed on the catalyst was removed by flushing the sample with helium (25 mL/min) for 1 h at the adsorption temperature. Thermal desorption of ammonia was carried out in the temperature range of 100–550 °C increasing at a rate of 10 °C/min. FTIR spectroscopy of pyridine adsorption measurements were performed on a Nicolet iS50 spectrometer equipped with a vacuum cell (Tuosi instrument Co., Ltd., Xiamen, China). Catalyst samples are pressed into self-supported wafers (10 ~ 15 mg with diameter of 13 mm) and activated under vacuum ( $1 \times 10^{-3}$  Pa) at 250 °C. After cooling to 100 °C, the samples were adsorbed to saturation with pyridine, and then vacuum treated at the same temperature to remove the physically adsorbed pyridine. Then the samples were heated to 450 °C at a rate of 10 °C/min, and the FTIR spectra were collected at 150 °C, 250 °C, 350 °C and 450 °C, sequentially. The spectra of the air background and pyridine adsorbed/desorbed samples were recorded with a spectral resolution of 4 cm<sup>-1</sup> in the region going from 400 to 4000 cm<sup>-1</sup>. The spectra so obtained are subtracted and processed with the Omnic software in order to obtain the adsorbed form. Transmission electron microscopy experiments were conducted on TECNAI G2 F30 operating at 300 kV. For the TEM image, the specimens were dispersed in ethanol and placed on holey copper grids.

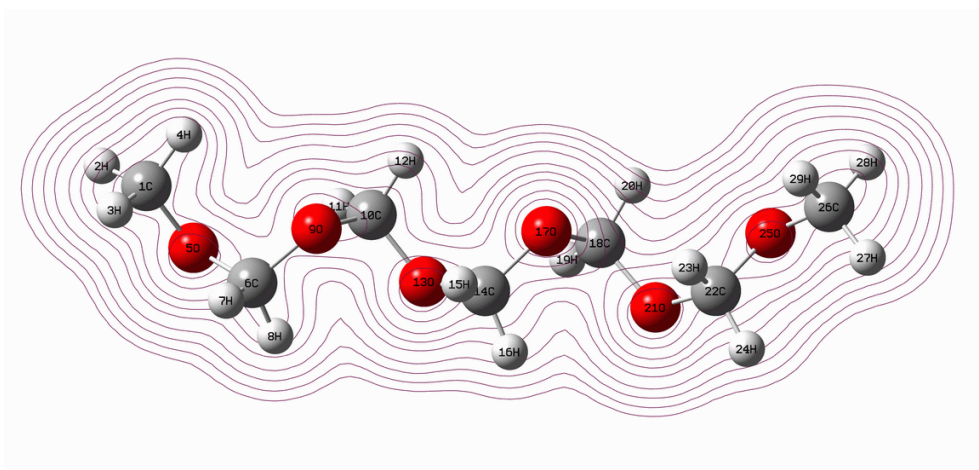


**Fig. S1**  $\text{CH}_3\text{O}(\text{CH}_2\text{O})_5\text{CH}_3$  model optimized using Gaussian 09.<sup>3</sup>

$\text{CH}_3\text{O}(\text{CH}_2\text{O})_3\text{CH}_3$  (PODE<sub>3</sub>),  $\text{CH}_3\text{O}(\text{CH}_2\text{O})_5\text{CH}_3$  (PODE<sub>5</sub>) and  $\text{CH}_3\text{O}(\text{CH}_2\text{O})_8\text{CH}_3$  (PODE<sub>8</sub>) models were optimized on B3LYP/6-311+g(d,p) level using Gaussian 09.<sup>3</sup> The optimization was carried out with a temperature at 378 K and a pressure at 1.3 MPa. The optimized model was used to demonstrate the size of PODE<sub>3</sub>, PODE<sub>5</sub> and PODE<sub>8</sub> and help to study the effect of pore size on catalytic performance. As an example, an optimized model of PODE<sub>5</sub> was illustrated in **Fig. S1** and all the optimized structures along with the sizes and energies were collected and summarized in **Table S3**.

### Reaction tests

The synthesis of PODE<sub>*n*</sub> was carried out in a Teflon-lined (100 ml) steel batch reactor. In a typical synthesis, the reactor was charged with freshly activated catalyst, trioxane and methylal. Then the reactor was purged three times with N<sub>2</sub> and pressurized. The mixture was heated and held at the elevated temperature for 2 h. After reaction, the reactor was cooled down and the mixture was centrifuged. The supernatant was collected and analyzed by gas chromatography (Techcomp GC-7900) using a flame ionization detector (FID) furnished with HP-5 60 m × 0.320 mm capillary column. In a typical analysis, 1 μL of the solution was injected into the GC from the inlet. The retention time interval of the products was longer than 1 min and the peak width was smaller than 0.3 min. The conversion was calculated based on the converted trioxane by using mesitylene as internal standard. And the product distribution was calculated using area normalization method. For recycling runs, the used catalyst was filtered, dried at 373 K overnight, calcined at 823 K for 5 h and reused in the next run.

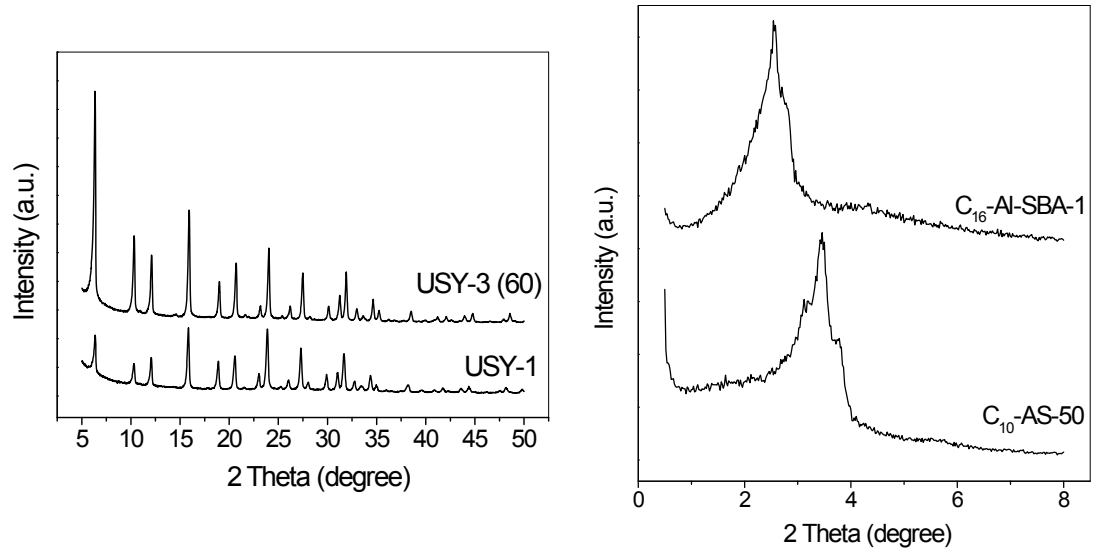


**Fig. S2** XRD patterns of the catalysts.

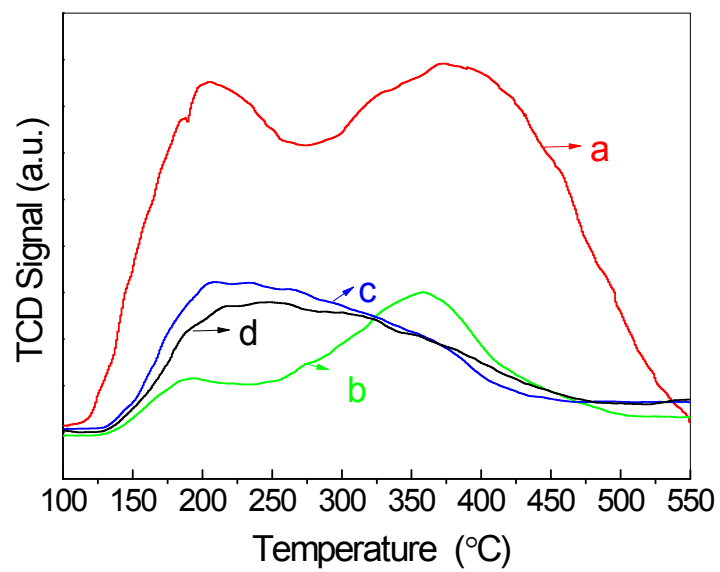


**Fig. S3** NH<sub>3</sub>-TPD profiles of aluminosilicate catalysts: (a) USY-1, (b) USY-3 (60), (c) C<sub>10</sub>-AS-50, and (d) C<sub>16</sub>-Al-SBA-1.

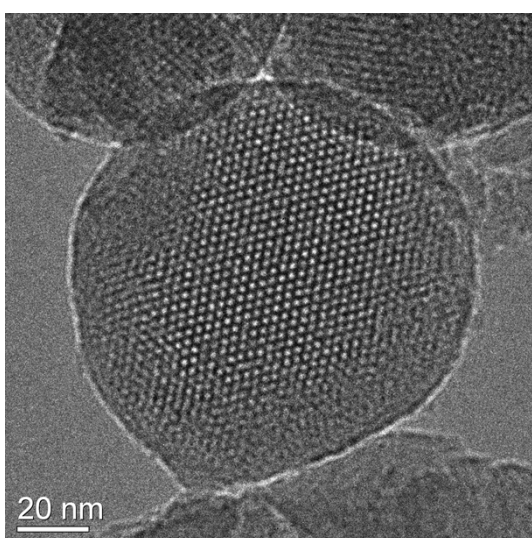
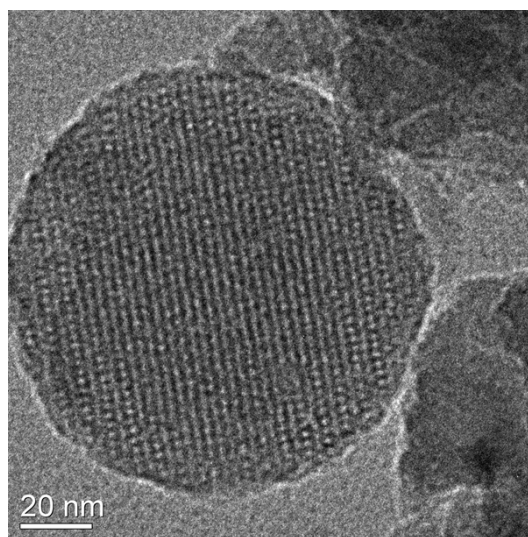
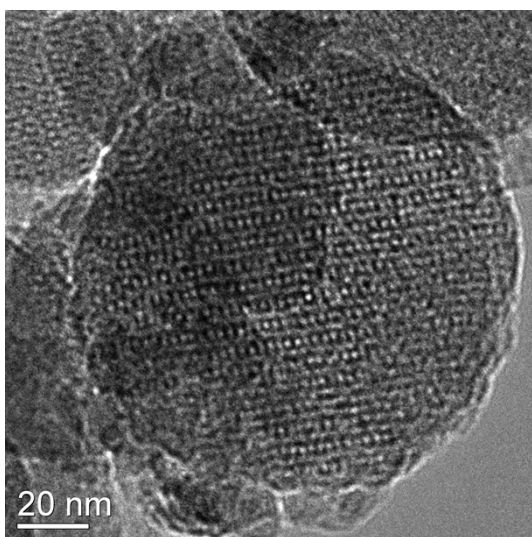


**Fig. S4** Typical transmission electron microscopy (TEM) images of C<sub>10</sub>-AS-50.



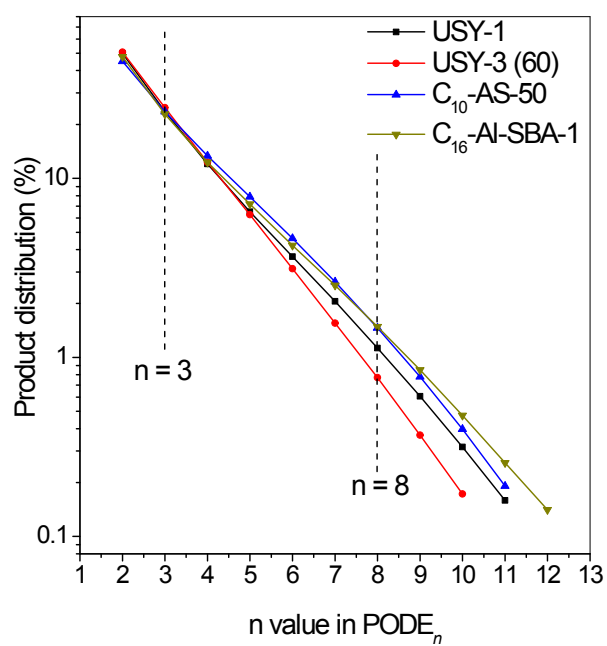


**Fig. S5** Product distribution versus the  $n$  value in  $\text{PODE}_n$  by using different catalysts.

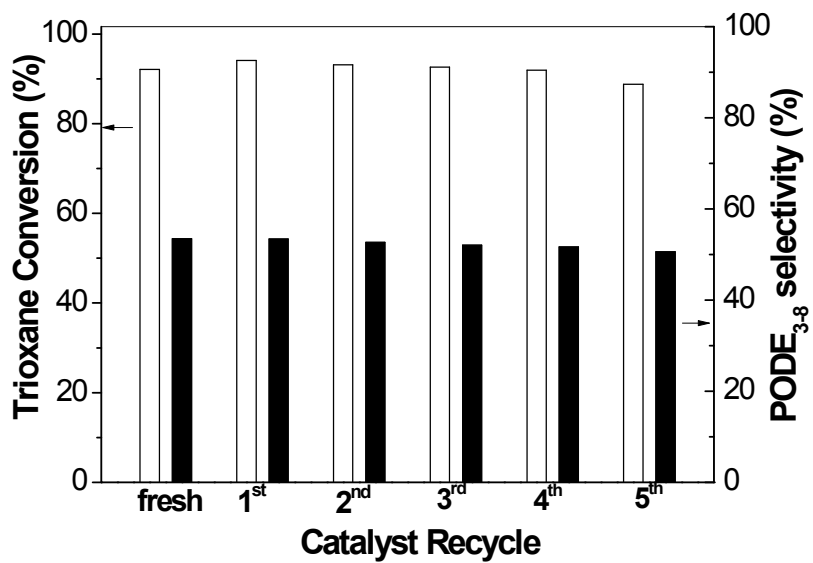


**Fig. S6** Recyclability studies of C<sub>10</sub>-AS-50 catalyst in the synthesis of PODE<sub>*n*</sub>.

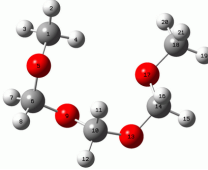
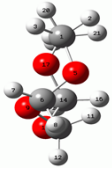
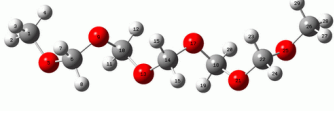
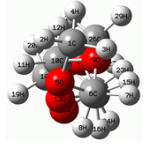
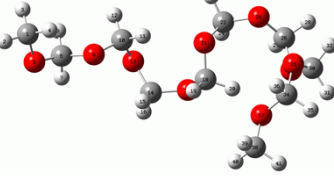
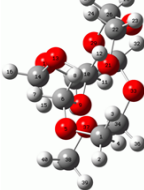
**Table S1** Physical properties of conventional diesel fuel (CDF), methylal and polyoxymethylene dimethyl ethers (PODE<sub>*n*</sub>).<sup>4</sup>

	CDF	methylal	PODE <sub><i>n</i></sub>				
			<i>n</i> = 2	<i>n</i> = 3	<i>n</i> = 4	<i>n</i> = 5	<i>n</i> = 6
Melting point (°C)	-	-105	-70	-43	-10	18.5	58
Boiling point (°C)	170-390	42	105	156	201	242	280
Viscosity (25 °C) (mPa s)	2.71	0.58	0.64	1.05	1.75		
Density liquid (25 °C) (kg/L)	0.83	0.860	0.960	1.024	1.067	1.10	1.13
Cetane number	55	29	63	70	90	100	104
Oxygen content (%)	-	42.1	45.3	47.1	48.2	49.0	49.6

**Table S2** PODE<sub>n</sub> product distribution by using different catalysts.

catalyst	PODE <sub>n</sub> product distribution										
	<i>n</i> = 2	<i>n</i> = 3	<i>n</i> = 4	<i>n</i> = 5	<i>n</i> = 6	<i>n</i> = 7	<i>n</i> = 8	<i>n</i> = 9	<i>n</i> = 10	<i>n</i> = 11	<i>n</i> = 12
USY-1	49.88	23.68	12.03	6.51	3.65	2.05	1.13	0.61	0.32	0.16	0.00
USY-3 (60)	50.60	24.84	12.30	6.27	3.13	1.56	0.77	0.37	0.17	0.00	0.00
C <sub>10</sub> -AS-50	45.07	23.58	13.35	7.90	4.63	2.65	1.46	0.78	0.40	0.19	0.00
C <sub>16</sub> -Al-SBA-1	47.74	22.84	12.28	7.19	4.22	2.52	1.48	0.85	0.47	0.26	0.14

**Table S3** The optimized models of PODE<sub>3</sub>, PODE<sub>5</sub> and PODE<sub>8</sub> by Gaussian 09.

PODE <sub>n</sub>	models after the optimization at B3LYP/6-311g +(d,p), 1.3 Mpa and 378 K		size of optimized models (a nm× b nm)*
	along major axis	perpendicular to major axis	
<i>n</i> =3			0.70 nm×0.52 nm
<i>n</i> =5			1.28 nm×0.32 nm
<i>n</i> =8			1.49 nm×0.28 nm

\*:

## References

1. W. H. Fu, S. J. Wu, Y. M. Wang and M. Y. He, *J. Mater. Chem. A*, 2014, **2**, 14908-14917.
2. M. J. Kim and R. Ryoo, *Chem. Mater.*, 1999, **11**, 487-491.
3. G. W. T. M.J. Frisch, H.B. Schlegel, G.E. Scuseria, M.A. Robb, J.R. Cheeseman, G. Scalmani, V. Barone, B. Mennucci, G.A. Petersson, H. Nakatsuji, M. Caricato, X. Li, H.P. Hratchian, A.F. Izmaylov, J. Bloino, G. Zheng, J.L. Sonnenberg, M. Hada, M. Ehara, K. Toyota, R. Fukuda, J. Hasegawa, M. Ishida, T. Nakajima, Y. Honda, O. Kitao, H. Nakai, T. Vreven, J.E.P. J.A. Montgomery Jr., F. Ogliaro, M. Bearpark, J.J. Heyd, E. Brothers, K.N. Kudin, V.N. Staroverov, R. Kobayashi, J. Normand, K. Raghavachari, A. Rendell, J.C. Burant, S.S. Iyengar, J. Tomasi, M. Cossi, N. Rega, N.J. Millam, M. Klene, J.E. Knox, J.B. Cross, V. Bakken, C. Adamo, J. Jaramillo, R. Gomperts, R.E. Stratmann, O. Yazyev, A.J. Austin, R. Cammi, C. Pomelli, J.W. Ochterski, R.L. Martin, K. Morokuma, V.G. Zakrzewski, G.A. Voth, P. Salvador, J.J. Dannenberg, S. Dapprich, A.D. Daniels, Ö. Farkas, J.B. Foresman, J.V. Ortiz, J. Cioslowski, D.J. Fox, *Gaussian, Inc. Wallingford, CT*, 2009.
4. a) B. Lumpp, D. Rothe, C. Pastötter, R. Lämmermann and E. Jacob, *MTZ Worldw*, 2011, **72**, 34-38; b) R. H. Boyd, *J. Polym. Sci.*, 1961, **50**, 133-141; c) J. Wu, Z. Xu, Z. Liu and B. Wang, *J. Chem. Eng. Data*, 2005, **50**, 966-968; d) M. Marchionna and R. Patrini. EP 1070755 B1, 2005.